Effect of dislocation scattering on the transport properties of InN grown on GaN substrates by molecular beam epitaxy

Kejia (Albert) Wang,[a] Yu Cao, John Simon, Jing Zhang, Alexander Mintairov, James Merz, Douglas Hall, Thomas Kosel, and Debdeep Jena
Department of Electrical Engineering, University of Notre Dame, Indiana 46556

(Received 10 July 2006; accepted 9 September 2006; published online 20 October 2006)

The authors report the structural, optical, and transport properties of high quality InN epitaxial films grown on GaN substrates by plasma-assisted molecular beam epitaxy. They have found a strong correlation between the structural quality and the measured carrier mobilities. Comparison of temperature-dependent Hall data with a theoretical transport model indicates that the electron mobility in state-of-art InN is limited by charged dislocation scattering. The model predicts that an order-of-magnitude increase in electron mobilities can be achieved by the reduction of dislocation densities in InN. © *2006 American Institute of Physics*. [DOI: 10.1063/1.2364456]

In recent years, InN has been extensively investigated for its electrical and optical properties because of its potential applications in high speed electronic devices and optical devices in the infrared (IR) region.[1–4] InN has a small electron effective mass [$0.05m_0$ (Ref. 5)] and high electron mobility. Monte Carlo simulations of the electron transport properties predict that the electron mobility in InN could reach 14 000 $cm^2/V\,s$ at room temperature and a peak drift velocity as high as 5×10^7 cm/s can be achieved.[6] The transport properties of electrons in InN are far superior to those in GaN; this stems from the narrow band gap, similar to InAs and InSb in the other III-V families. In recent work, it has been reported that the fundamental band gap of InN is around 0.7 eV,[7] and thus the III-V nitrides semiconductor family is the only material system whose band gaps span from the ultraviolet (UV) (AlN at 6.2 eV) through the visible to the IR (InN at 0.7 eV) region. Since the their band gaps can cover the entire solar spectrum and they have been proven to be radiation hard,[8] they can be used for high efficiency photovoltaic applications with environment-friendly nontoxic elements, both for terrestrial and space applications.

The many applications mentioned above require high quality crystalline InN with a high degree of structural integrity, and good optical and electrical properties. However, the growth of InN presents a challenge because of its low dissociation temperature, the high equilibrium vapor pressure of nitrogen molecules, and the lack of a suitable substrate.[4] Recently, high quality InN has been grown on sapphire substrates by both metal organic chemical vapor deposition[9] (MOCVD) and molecular beam epitaxy (MBE).[10,11] However, few groups have reported a relation between the structural, optical, and transport properties of InN on GaN substrates.

In this work, we have studied the MBE growth of InN directly on GaN substrates. The structural quality of grown InN has been characterized by reflection high energy electron diffraction (RHEED), x-ray diffraction (XRD), transmission electron microscope (TEM), and atomic force microscopy (AFM). We have also measured the transport properties of carriers in InN by temperature-dependent Hall measurements and extracted the scattering mechanisms limiting the mobility. Optical properties have been characterized using photoluminescence spectroscopy. Finally, we find a strong correlation between the structural and transport properties of the as grown InN layers, and identify charged dislocation scattering as the dominant scattering mechanism.

A Veeco Gen 930 MBE system with a Veeco UNI-Bulb rf plasma source configured for the growth of III-V nitrides was used for the growth of InN. Commercially available semi-insulating GaN-on sapphire templates were used in this work as the substrate. A two-step growth process was used: an thin InN buffer layer (about 60 nm) was grown at a low substrate temperature (360 °C), followed by an epitaxial InN layer at a higher substrate temperature (510 °C). During the growth, *in situ* RHEED was used to monitor the evolution of the surface morphology of the InN film. After the growth, the samples were examined under an optical microscope to determine if there were excess indium metal droplets on the sample surface; if present they were removed by HCl treatment. Four InN samples were grown at different indium fluxes (Table I). Sample A was grown in the nitrogen-rich regime (III/V ratio <1) and no metal droplets were observed on the surface after growth. Sample B was grown in a slightly In-rich regime and only a few In droplets were observed. Samples C and D were grown at higher indium flux and after growth there were In droplets left on the surface. Surface morphology of InN sample was characterized by AFM. The root-mean-square (rms) surface roughnesses of the four InN samples for a 2×2 μm^2 scan are listed in Table I. All four samples were grown for 2 h with a total thickness of 710 nm.

A cross-section TEM specimen of sample C was prepared by mechanical wedge polishing and ion milling at 2 keV with liquid nitrogen cooling. TEM investigation was carried out using a JEOL 2010 system with 200 kV accelerating voltage. A high resolution TEM lattice image of InN is shown in Fig. 1(b). The *c*-lattice constant measured from the lattice image is 5.63 Å. The bright field image shown in Fig. 1(a) was taken near $g=0002$, which would put edge-type threading dislocations with Burgers vectors $b=a$ out of contrast. The observed threading dislocations are thus of screw type ($b=c$) or mixed ($b=c+a$). These are observed to originate at the InN/GaN interface and propagate towards the surface. The total dislocation density is estimated to be about 4×10^{11} cm^{-2}, and the average distance between each dislocation is about 16 nm.

[a]Electronic mail: kwang@nd.edu

TABLE I. Structural and electrical characterizations of samples A–D grown at different In fluxes: surface roughness (rms) measured by AFM, FWHM of (0002) peak in ω scan, room temperature and 77 K mobility (μ), sheet carrier concentration (n_s), and effective carrier volume concentration (n_v). The effective carrier volume concentration is calculated considering a surface charge of 2.4×10^{13} cm^{-2} near the InN surface (Ref. 12).

Sample	In flux 10^{-7} torr	rms (nm)	FWHM (deg)	RT mobility (cm^2/V s)	RT n_s ($\times10^{14}$ cm^{-2})	n_v ($\times10^{18}$ cm^{-3})	77 K mobility (cm^2/V s)	77 K n_s ($\times10^{14}$ cm^{-2})
A	3.1	9.52	0.4623	943	3.11	4.04	1009	3.02
B	3.2	6.64	0.5749	782	3.12	4.06	809	3.07
C	3.29	0.82	0.42	1054	3.02	3.92	1154	2.89
D	3.39	2.53	0.4612	984	3.08	4.00	1036	2.99

High resolution x-ray diffraction (HRXRD) was used to characterize the epitaxial film quality and to measure the *c*-axis lattice constant. The HRXRD measurements were taken with a Panalytical X'pert Pro MRD system. Figure 2 shows the (0002) $\omega/2\theta$ scans of InN grown on GaN. A wurtzite structure InN (0002) peak is clearly observed. Taking the lattice constant (*c* axis) of GaN to be 5.186 Å, the lattice constant (*c* axis) of InN is calculated to be 5.694 Å. This is close to the reported value of 5.693 Å (Ref. 13) and slightly higher than estimated from the TEM lattice image. The insert in Fig. 2 shows the ϕ scan of the (012) plane of InN. It shows six peaks separated by 60°, confirming the sixfold symmetry of the wurtzite structure. In the ω scan, the XRD peak is broadened due to the mosaicity, lateral incoherence, dislocations, and sample curvature. We compare the full width at half maximum (FWHM) of (0002) ω rocking curve scans for the four samples in Table I to characterize the structural quality. Sample C is observed to have the smallest peak broadening. Thus from AFM and XRD analyses, it is clear that sample C has the best structural quality, followed by samples D, A, and B.

To investigate the role of structural defects and unintentional impurities on electron transport properties in bulk InN, Hall measurements were performed. The samples were cut into square pieces, and indium dots were used to form Ohmic contacts in the van der Pauw geometry. A magnetic field of 0.3 T was used. Room-temperature (RT) measurements were performed on all samples; the measured low-field mobilities and the sheet carrier concentrations are shown in Table I. The carrier mobilities lie in the 780–1050 cm^2/V s range at RT and improve marginally to 800–1150 cm^2/V s range at 77 K, while the integrated sheet carrier concentration stays around $n_s\sim3\times10^{14}$/cm^2 for all samples (this corresponds to a free-electron volume density of roughly $n_v\sim4\times10^{18}$/cm^3 neglecting the surface accumulation layer[12]). It is evident that there is a strong correlation between the structural quality (the FWHM values in Table I and the measured carrier mobilities. Sample C with the lowest FWHM in the ω scans along the (0002) axis demonstrates the highest mobility, followed by samples D, A, and B. This observation hints that dislocations might be important in determining the nature of electron transport in InN. To investigate the role of various scattering mechanisms on the electron mobility, temperature-dependent Hall measurements from 8 to 300 K were performed in a closed-cycle cryostat. All four samples exhibited similar behavior; the results for sample D are discussed here.

Figure 3(a) shows the measured Hall mobility and sheet carrier density over the temperature range. Considering the small electron effective mass in InN and the low conduction band density of states, the Fermi level in InN is expected at an energy $E_F-E_C=\hbar^2k_F^2/2m^*\approx180$ meV *above* the conduction band edge E_C [here $k_F=(3\pi^2n_v)^{1/3}$ is the Fermi wave vector and n_v is the measured volume density of electrons]. It is evident from the measurement that the free-electron density changes little with temperature, demonstrating that the carriers are degenerate. Therefore, one can make the assumption that the Hall mobility and drift mobility are identical,[14] since the Hall coefficient for degenerate carrier transport is $R_H=1$. Using this approximation, we calculate the contributions of various scattering mechanisms to the total mobility; the results are shown in Fig. 3(b) along with the measured values. Details of the calculation will be published in a separate work; here we mention our main observations.

Polar optical phonons, acoustic phonons (both deformation potential and piezoelectric modes), ionized impurities, and charged dislocation scattering are considered in the calculation, and their individual contributions to the total mobility are shown in Fig. 3(b). A dislocation density of $N_{\rm dis}=7.8\times10^{10}$/cm^2 was used with a filling fraction $f=1$, and the charge-neutrality condition was used for estimating the unintentional acceptor density $N_A\approx6\times10^{17}$/cm^3 for the best fit to the measured data. It is clear that not all the dislocations imaged by TEM can be charged; a similar observation was made by Look *et al.* based on charge neutrality conditions in

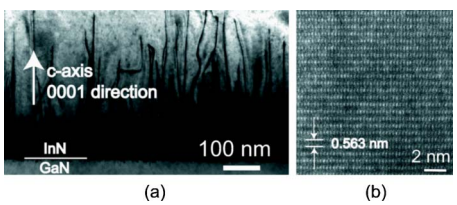

FIG. 1. (a) Bright field cross-section TEM image of InN on GaN. (b) High resolution TEM lattice image of InN.

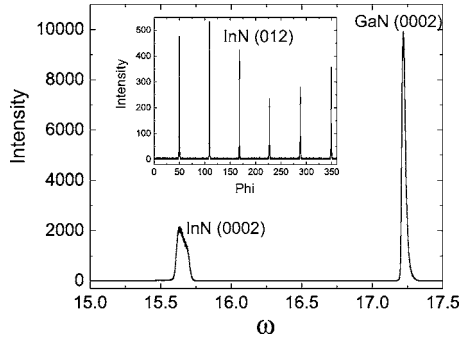

FIG. 2. XRD (002) ω-2θ scan of InN grown on GaN/sapphire substrate. The insert shows the ϕ scan of (012) plane in InN.

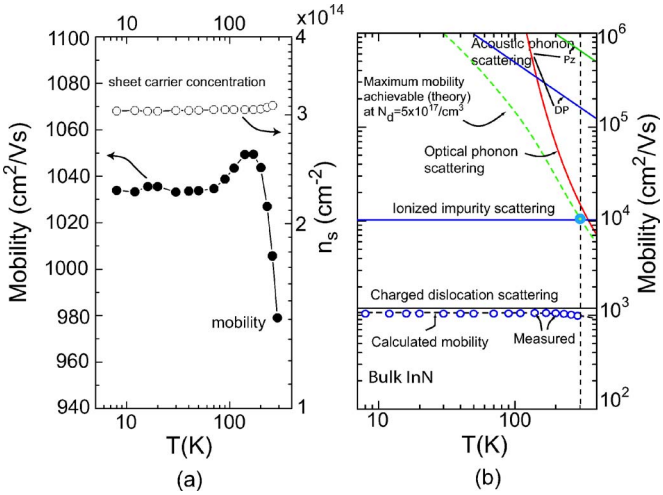

FIG. 3. (Color online) Temperature-dependent Hall data of InN. (a) Mobility and integrated electron sheet density vs temperature for sample D. (b) Comparison of measured mobility with a theoretical transport model. Charged dislocation scattering is identified as the dominant mobility-limiting scattering mechanism. If dislocation densities and background ionized impurity densities could be reduced, RT mobilities as high as 10 000 cm^2/V s can be achieved.

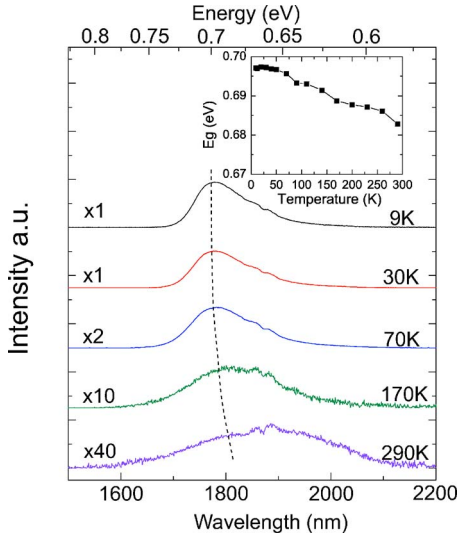

FIG. 4. (Color online) Temperature dependent photoluminescence spectra of InN (sample C). Insert: photoluminescence peak positions at different temperatures.

an earlier work.[15] From the calculations, we conclude that dislocation scattering is the dominant scattering mechanism in our samples over the *entire* temperature range, followed by ionized impurity scattering. The strong correspondence of transport properties with the measured structural quality (FWHM in x ray) supports this conclusion. It can safely be predicted that in dislocation-free InN, at an ionized impurity density of $N_d=5\times10^{17}/cm^2$ RT mobilities approaching 10 000 cm^2/V s. limited intrinsically by polar optical phonon scattering can be achieved, as shown in the theoretical plot in Fig. 3(b). This offers a major motivation for improving the epitaxial quality of InN, aimed at reduction of dislocation densities for the various device applications mentioned earlier.

The InN layers grown were optically characterized using photoluminescence spectroscopy. All InN samples grown by MBE were visibly dark, and the surfaces were mirror-like and shiny. The photoluminescence spectrum of InN was measured using a single-grating monochromator and a PbS detector, which has a band gap of 0.41 eV. The InN sample was pumped by an Ar^+ laser at 514 nm with power intensity of 100 W/cm^2 At room temperature, we observed an InN peak at 0.68 eV, which is close to recently reported work.[16,17] To measure the low-temperature photoluminescence spectra, the sample was held in a closed-cycle He refrigerator. Temperature dependent photoluminescence spectra are plotted in Fig. 4. As the temperature increased from 9 K to room temperature, the photoluminescence intensity is observed to decrease by about 20 times. The peak positions slightly shift to shorter wavelength as the temperature decreases (insert of Fig. 4). No peaks around 1.9 eV have been observed from 8 to 300 K, corroborating earlier observations that the fundamental band gap of InN is ~0.69 eV.

In conclusion, high quality InN epitaxial layers grown on GaN substrate by MBE were demonstrated. A close correlation was found between the structural quality of InN and the electron transport properties. The mobility of electrons in state-of-the-art InN epilayers was found to be limited by charged dislocation scattering by a combined experimental and theoretical analysis. The optical band gap was found to be ~0.69 eV, and little variation with temperature (8–300 K) was observed. It is predicted that with improvements in epitaxial growth techniques resulting in reduction of dislocation densities, room temperature electron mobilities as high as 10 000 cm^2/V s can be achieved for InN, making the material extremely attractive for a member of device applications.

The authors would like to thank C. Wood (ONR) and Kitt Reinhardt (AFOSR) for support and useful discussions.

[1]H. Lu, W. J. Schaff, J. Hwang, H. Wu, W. Yeo, A. Pharkya, and L. F. Eastman, Appl. Phys. Lett. **77**, 2548 (2000).
[2]H. Lu, W. J. Schaff, L. F. Eastman, and C. E. Stutz, Appl. Phys. Lett. **82**, 1736 (2003).
[3]J. Wu, W. Walukiewicz, W. Shan, K. M. Yu, J. W. Ager III, S. X. Li, E. E. Haller, H. Lu, and W. J. Schaff, J. Appl. Phys. **94**, 4457 (2003).
[4]Y. Nanishi, Y. Saito, and T. Yamaguchi, Jpn. J. Appl. Phys., Part 1 **42**, 2549 (2003).
[5]S. P. Fu and Y. F. Chen, Appl. Phys. Lett. **85**, 1523 (2004).
[6]V. M. Polyakov and F. Schwierz, Appl. Phys. Lett. **88**, 032101 (2006).
[7]V. Yu. Davydov, A. A. Klochikhin, R. P. Seisyan, V. V. Emtsev, S. V. Ivanov, F. Bechstedt, J. Furthmuller, H. Harima, A. V. Mudryi, J. Aderhold, O. Semchinova, and J. Graul, Phys. Status Solidi B **229**, R1 (2002).
[8]J. Wu and W. Walukiewicz, Superlattices Microstruct. **34**, 63 (2003).
[9]A. Yamamoto, T. Tanaka, K. Koide, and A. Hashimoto, Phys. Status Solidi A **194**, 510 (2002).
[10]Y. Saito, T. Yamaguchi, H. Kanazawa, K. Kano, T. Araki, Y. Nanishi, N. Teraguchi, and A. Suzuki, J. Cryst. Growth **237–239**, 1017 (2002).
[11]Hai Lu, William J. Schaff, Jeonghyun Hwang, Hong Wu, Goutam Koley, and Lester F. Eastman, Appl. Phys. Lett. **79**, 1489 (2001).
[12]I. Mahboob, T. D. Veal, L. F. J. Piper, C. F. McConville, H. Lu, W. J. Schaff, J. Furthmller, and F. Bechstedt, Phys. Rev. B **69**, 201307 (2004).
[13]A. Zubrilov, *Properties of Advanced Semiconductor Materials GaN, AlN, InN, BN, SiC, SiGe* (Wiley, New York, 2001), p. 49.
[14]K. Seeger, *Semiconductor Physics*, 9th ed. (Springer, Berlin, 2004), p. 59.
[15]D. C. Look, H. Lu, W. J. Schaff, J. Jasinski, and Z. Liliental-Weber, Appl. Phys. Lett. **80**, 258 (2002).
[16]K. M. Yu, Z. Liliental-Weber, W. Walukiewicz, W. Shan, J. W. Ager III, S. X. Li, R. E. Jones, E. E. Haller, Hai Lu, and William J. Schaff, Appl. Phys. Lett. **86**, 071910 (2005).
[17]Y. Nanishi, Y. Saito, T. Yamaguchi, T. Araki, T. Miyajima, and H. Naoi, Phys. Status Solidi C **1**, 1487 (2004).